Catalysis Today 150 (2010) 340–345

Contents lists available at ScienceDirect

Catalysis Today

journal homepage: www.elsevier.com/locate/cattod

Calcined layered double hydroxides Mg–*Me*–Al (*Me*: Cu, Fe, Ni, Zn) as bifunctional catalysts

Jaime S. Valente *, Jose Hernandez-Cortez, Manuel S. Cantu, Gerardo Ferrat, Esteban López-Salinas

Instituto Mexicano del Petróleo, Eje Central # 152, 07730 México, D. F., Mexico

ARTICLE INFO

Article history:
Available online 26 September 2009

Keywords:
Layered double hydroxides
4-Methylpentan-2-ol conversion
Redox properties
Bifunctional catalysts

ABSTRACT

A series of layered double hydroxides (LDHs) materials containing different divalent and trivalent cations $[Mg_{1-x-y}Me_xAl_y(OH)_2](CO_3)_{y/2}\cdot mH_2O$, where *Me*: Cu, Fe, Ni, Zn; were prepared by coprecipitation. The solids were characterized by X-ray diffraction, temperature-programmed reduction (TPR) and temperature-programmed desorption (TPD) of CO_2; thermogravimetric and textural analysis were also performed. All solids, dried at 100 °C, showed XRD patterns typical of hydrotalcite, where *Me* cations isomorphically replaced some Mg^{2+} cations within the layers, thus forming a ternary LDH, as the starting material. The materials were calcined at 550 °C and tested as catalysts in the gas-phase conversion of 4-methylpentan-2-ol at 200 °C.

1. Introduction

Throughout previous decades, layered double hydroxides (LDHs), also known as hydrotalcite-like compounds, have been extensively studied as catalysts or catalyst precursors [1]. Since calcination of LDHs yields mixed oxides with basic properties, LDHs have found applications in many organic reactions considered to be catalyzed by bases [1–3]. The structure of LDHs resembles that of brucite, $Mg(OH)_2$, in which magnesium is octahedrally coordinated to hydroxyls. By sharing edges, $Mg(OH)_2$ octahedra form infinite layers. Replacing some of the divalent cations by trivalent cations results in an LDH structure, in which the layered array is positively charged. These positively charged double hydroxide layers are electrically compensated by anions which are located in the interlayer region. As a wide variety of synthetic LDHs can be prepared, they are represented by the general formula: $[M_{(1-x)}^{2+}M_x^{3+}(OH)_2]^{x+}(A^{n-})_{x/n}\cdot mH_2O$, where $M^{2+} = Mg^{2+}$, Ni^{2+}, Cu^{2+}, Zn^{2+}, etc.; $M^{3+} = Al^{3+}$, Fe^{3+}, Ga^{3+}, etc.; $A^{n-} = [CO_3]^{2-}$, Cl^-, $[V_{10}O_{28}]^{6-}$, etc.

The most common LDH, MgAl, can be used to incorporate and disperse one or more reducible transition metal cations *Me* in the layers, when partially replacing Mg^{2+} and/or Al^{3+} cations; the layers then have the general formula $[Mg_{1-x-y}Me_xAl_y(OH)_2]$. These reducible cations, when they are indeed located in the layers and not as separate metal hydroxide or oxide entities, are imbedded in a mostly basic matrix. The transition metal may also induce a certain degree of acidity. Accordingly, it is possible to modulate the basic strength of a series of ternary layered double hydroxide clays, depending on the nature of the cations in the layers [4].

It is well known that, when a bimetallic LDH is calcined, the layered array collapses, and a solid solution is obtained, where the only crystalline phase is that of the oxide in larger proportion (e.g. MgO from a MgAl LDH), the second cation being highly dispersed. In LDHs containing three or more cations, the same phenomenon is observed. Mixed oxides containing highly disperse, small crystals of the reducible metal oxides may show interesting catalytic properties [5]. In this sense, LDHs with three or more cations, e.g. Mg–Zn–Al and Zn–Cu–Al [6], Ni–Al–Cr and Ni–Al–Fe [7] and Cu–Mg–Al [8], incorporated in the layers have been reported, but they have scarcely been applied as catalysts.

Conversion of 4-methylpentan-2-ol has been studied with a view to throw light on the acid–base properties of a variety of solid catalysts [9–13]. This reaction is catalyzed by materials containing both acid and base sites. Acid sites catalyze dehydration reactions, while basic sites catalyze dehydrogenation reactions (Scheme 1). In fact, this reaction has been used to characterize the relative population of weak, intermediate and strong acid sites on a given catalyst [9]. For instance, the primary product of dehydration, 4-methylpent-1-ene (4MP1ene) is formed on weak acid sites, while 4-methylpent-2-ene (4MP2ene) requires intermediate acid strength. All other products in this reaction, where the methyl group migrates to other parts of the molecule (i.e. skeletal isomerization), need very strong acid sites. The dehydrogenation route, however, which yields 4-methylpentan-2-one (MIBK), has been ascribed exclusively to basic sites [9]. The dehydrogenation route could be enhanced by the inclusion of reducible cations on the catalysts.

* Corresponding author at: Instituto Mexicano del Petróleo, Eje Central # 152, 07730 México, D. F., Mexico. Tel.: +52 55 9175 8444.
E-mail addresses: jsanchez@imp.mx, sanchezvalente@yahoo.com (J.S. Valente).

0920-5861/$ – see front matter © 2009 Elsevier B.V. All rights reserved.
doi:10.1016/j.cattod.2009.08.020

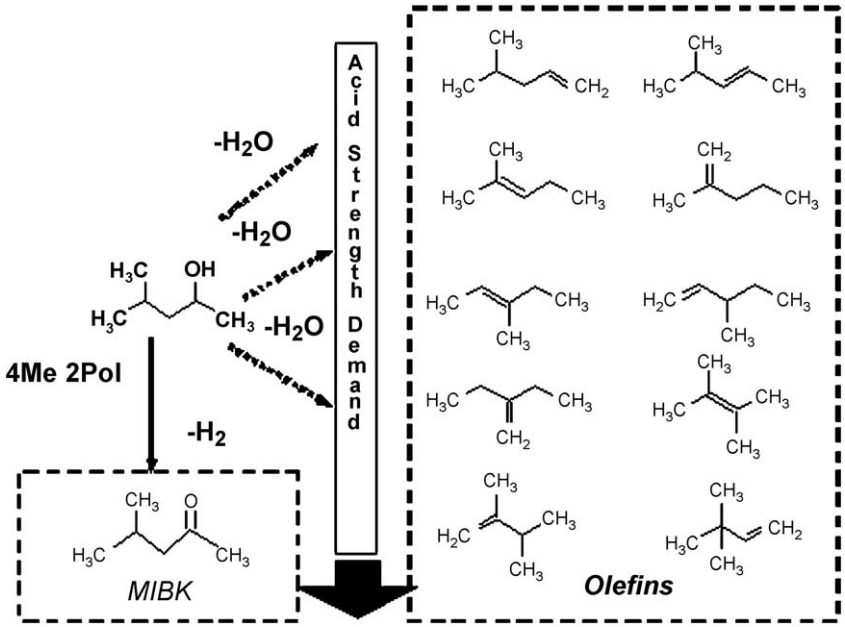

Scheme 1. Conversion of 4-methylpentan-2-ol: dehydration and dehydrogenation routes.

Indeed, many efforts have been devoted to produce selectively MIBK directly from acetone, avoiding secondary reactions (e.g. dehydrations and successive ketone condensations); this issue remains a huge challenge of fine tuning acid–base and hydrogenating properties on prospective catalysts [14].

With a view to examine the effect of introducing transition metals on acid–base and redox properties of MgAl LDHs, a series of LDHs $[Mg_{1-x-y}Me_xAl_y(OH)_2]\ (CO_3)_{y/2}\cdot mH_2O$; *Me* = Cu, Fe, Ni, Zn; were synthesized, characterized and calcined; and then tested as catalysts in the gas-phase conversion of 4-methylpentan-2-ol. MgAl LDH was also tested as a comparison.

2. Experimental

2.1. Catalyst preparation

The layered double hydroxides were prepared by coprecipitation following a procedure described elsewhere [15]. All samples, except for that containing Fe^{3+}, were prepared as follows.

A 1 M aqueous solution containing the nitrates of the metallic salts (solution A) was prepared. A M^{2+}/M^{3+} molar ratio of 3 was established in all cases. Separately, an aqueous solution containing KOH and/or K_2CO_3 (solution B) was prepared. Solutions A and B were added drop wise simultaneously into a glass reactor, maintaining the slurry's final pH between 8 and 10, depending on the chemical composition. The slurry was aged at 65 °C for 18 h under vigorous stirring. MgCuAl sample was aged only for 30 min. The precipitate was washed several times with hot deionized water and dried at 100 °C overnight.

Although MgFeAl LDH can be prepared by the procedure describe above, obtaining MgFeAl with pure LDH phase can only be achieved by coprecipitation at high supersaturation, as reported by other authors [16,17]. The same consideration is applicable to NiFe synthesis [18]. Therefore, MgFeAl sample was synthesized as follows: a 1 M solution containing $Mg(NO_3)_2\cdot 6H_2O$, $Al(NO_3)_3\cdot 9H_2O$ and $Fe(NO_3)_3\cdot 9H_2O$ (solution A), and a 2 M solution containing KOH and K_2CO_3 (solution B) were prepared. A M^{2+}/M^{3+} molar ratio of 3 was established. Solution B was added dropwise to solution A until a pH ~ 8 was attained. The resulting slurry was aged at 65 °C for 18 h under a vigorous stirring. The precipitate was washed several times with hot deionized water and dried at 100 °C overnight.

2.2. Characterization methods

Chemical composition of solids was determined in a Perkin Elmer Mod. OPTIMA 3200 Dual Vision by inductively coupled plasma atomic emission spectrometry (ICP-AES).

The X-ray diffraction patterns of the samples were measured in a Siemens D-500 diffractometer with Cu $K\alpha_1$ radiation. Diffraction intensity was measured between 4° and 80°, with a 2θ step of 0.02° and a counting time of 9 s per point.

Thermogravimetric analyses were carried out using Perkin-Elmer TG-7. Samples were heated in flowing anhydrous air (20 mL min^{-1}) from room temperature to 800 °C, with a constant heating rate of 10 °C min^{-1}.

Surface areas, pore volume and pore size distribution of the samples calcined at 550 °C were obtained from the N_2 adsorption–desorption isotherms determined at −196 °C on a Quantachrome Autosorb-1C equipment. Surface area was calculated by using BET equation and pore size distribution was calculated by the BJH method using the desorption branch.

Temperature-programmed reduction (TPR) and temperature-programmed desorption (TPD) of CO_2 measurements were carried out in a Quantachrome Autosorb-1C equipment with an on-line quadrupole mass spectrometer (PRISMA-QMS 200). For the TPR analysis, the reducing agent was a hydrogen–nitrogen mixture (10 mol% H_2). This was used to reduce the sample (~100 mg) at a flow rate of 10 mL min^{-1}. The temperature was linearly raised at a rate of 5 °C min^{-1} up to 650 °C. The gas mixture was analyzed by a mass spectrometer of Pfeiffer Prisma. Calibration of the instrument was carried out with CuO (from Merck). On the other hand, TPD-CO_2 was carried out on 100 mg sample, under helium as carrier gas (flow rate 25 mL h^{-1}). Prior to CO_2 adsorption, all catalysts were heated up to 650 °C. Samples were then cooled to 50 °C, and exposed to a flow of CO_2 for 1 h. Desorption proceeded by heating (10 °C min^{-1}) up to the final temperature of 650 °C.

2.3. Catalytic reaction

All solids were evaluated as catalysts in the gas-phase conversion of 4-methylpentan-2-ol. This reaction was carried out in a fix-bed quartz tubular reactor fed by He (as a carrier gas). All stainless steel tubing in and out of the reactor was heated at 150 °C in order to avoid

Table 1
Chemical formulas, cell parameters and average crystal sizes of the LDHs.

Sample	Chemical formula	M^{2+}/M^{3+}	a (Å)	c (Å)	$L_{0\,0\,3}$[a] (Å)	$L_{1\,1\,0}$[a] (Å)
MgAl	$[Mg_{0.751}Al_{0.248}(OH)_2]\ (CO_3)_{0.124}\cdot 0.74H_2O$	3.03	3.056	23.34	106	212
MgFeAl	$[Mg_{0.650}Fe_{0.063}Al_{0.286}(OH)_2]\ (CO_3)_{0.175}\cdot 0.74H_2O$	1.86	3.076	23.04	153	191
MgNiAl	$[Mg_{0.547}Ni_{0.120}Al_{0.333}(OH)_2]\ (CO_3)_{0.166}\cdot 0.93H_2O$	2.00	3.043	22.79	102	152
MgCuAl	$[Mg_{0.658}Cu_{0.098}Al_{0.244}(OH)_2]\ (CO_3)_{0.122}\cdot 0.69H_2O$	3.09	3.069	22.93	72	101
MgZnAl	$[Mg_{0.614}Zn_{0.093}Al_{0.293}(OH)_2]\ (CO_3)_{0.147}\cdot 0.75H_2O$	2.41	3.058	23.18	125	236

[a] Crystal sizes calculated by the Scherrer equation on the 0 0 3 and 1 1 0 reflections.

condensation. The reaction conditions were: 200 °C, WHSV = 8.32 × 10^{-3} h^{-1} (W/F = 0.0807 g_{cat} h g_{react}^{-1}), atmospheric pressure, He/4-methylpentan-2-ol = 39.303 molar, 28.0 mg of 80/100 mesh catalyst (except where indicated). The solid catalysts were all heat treated *in situ* at 500 °C for 1 h using He or Air in order to purge all gaseous impurities off the catalyst surface, and then they were brought to reaction temperature. In indicated runs, air instead of He, was used as the carrier gas with the purpose of studying the effect of an oxidative atmosphere in the products distribution. The reaction products were analyzed on-line by means of an automatic six-port sampling valve, connected to a Varian Star 3600 CX Gas-Chromatograph, equipped with a Flame Ionization Detector. A 50 m capillary PONA column was used to separate the products.

3. Results and discussion

3.1. Characterization of the fresh and calcined hydrotalcites

Elemental chemical analysis data of the LDH samples determined by ICP-AES are summarized in Table 1. The M^{2+}/M^{3+} molar ratios varied from 1.86 for MgFeAl to 3.09 for MgCuAl. Fig. 1 shows the XRD powder patterns of the LDHs dried at 100 °C, where all samples presented the characteristic reflections corresponding to layered double hydroxide structure, and no different crystalline phases were detected.

Crystal sizes (L) were calculated on the 0 0 3 and 1 1 0 reflections, using the Scherrer equation (Table 1). The unit cell parameters (see Table 1) were calculated assuming a 3R stacking sequence, that is, $a = 2d_{1\,1\,0}$ and $c = 3d_{0\,0\,3}$. Accordingly, the c parameter is related to the interlayer thickness, and is regulated by water content along with the amount, size, orientation, and charge of the anions located between the brucite-like layers, and the cell parameter a is the average cation–cation distance inside the brucite-like layers [19].

When the isomorphic substitution of a M^{2+} or a M^{3+} cation is performed, the cell parameter a may increase or decrease; this variance will depend mainly on the ionic radii of the cations in octahedral coordination, which decreases in the following order: $Zn^{2+} > Cu^{2+} > Mg^{2+} > Ni^{2+} > Fe^{3+} > Al^{3+}$. Thus, a simple way to confirm the isomorphic substitution of divalent and/or trivalent cations is by analyzing the variation of the cell parameter a. For instance, in Table 1, MgFeAl, MgZnAl and MgCuAl have larger a parameter values than that of MgAl. These results can be rationalized considering that the ionic radius of Fe^{3+} is larger than that of Al^{3+}, and Zn^{2+} and Cu^{2+} are bulkier than Mg^{2+}. On the other hand, MgNiAl has the smallest value of the series, which is also in agreement with the ionic radii of the cations.

The differences in c parameters between various LDHs can be attributed to the different coulombic attractive forces between the positively charged brucite-like layer and the anion located in the interlayer region. The excess of positive charge is caused by the isomorphic substitution of the different M^{2+} and M^{3+} cations [1,19,20]. Introducing a cation with higher electronegativity will increase the strength of said attractive forces, and decrease interlayer distances. The electronegativity of the M^{2+} cations increases in the following order $Mg < Al < Zn < Ni \sim Fe < Cu$. Assuming all LDHs having the same charge compensating anions (CO_3^{2-}), then interlayer distances should decrease upon increasing electronegativity of cations. Accordingly, MgAl has the largest c parameter.

Fig. 2 exhibits the XRD patterns of the samples calcined at 550 °C for 4 h. It is well known that when an LDH is calcined below 700 °C, only the metal oxide of the metallic cation present in major amount will be detected [21]. Accordingly, in all samples only a poorly crystallized MgO phase was obtained. However, in MgCuAl, a CuO phase (JCPD 01-078-0428) was detected, besides MgO. The feasibility of obtaining a metallic oxide of the third cation (in this case, CuO) at lower temperatures than in the other trimetallic samples, can be explained by the known Jahn–Teller effect of the copper ions [1], and their behavior inside the brucite-like layers [22]. Crystal sizes of the calcined samples were 61, 64, 65 and 66 Å, for MgCuAl, MgNiAl, MgZnAl and MgFeAl, respectively, calculated from the 1 0 0 reflection.

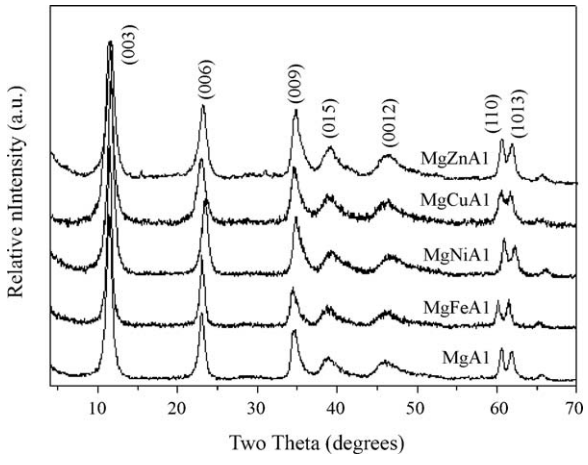

Fig. 1. Powder X-ray diffraction patterns of the layered double hydroxide compounds.

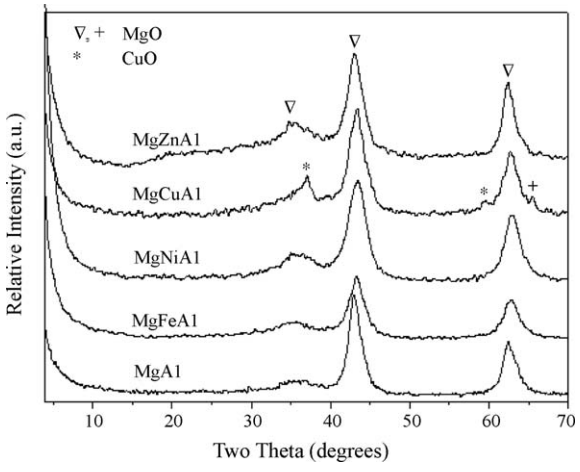

Fig. 2. Powder X-ray diffraction patterns of the mixed oxides obtained after thermal treatment at 550 °C of the LDHs.

Table 2
Results of the thermogravimetric analysis of LDHs.

Samples	Temperature intervals			Total weight loss (%)
	50–250 °C	250–450 °C	450–650 °C	
MgAl	18.7	22.9	3.5	45.1
MgFeAl	16.0	21.1	4.1	41.2
MgNiAl	17.5	21.4	3.6	42.5
MgCuAl	14.5	24.2	4.3	43.0
MgZnAl	15.6	19.9	5.8	41.3

Results from thermogravimetric analyses are shown in Table 2. The samples lost between 41.2 and 45.1 wt%. In general, LDH decomposition occurred at variable temperatures depending on their chemical composition. However, in order to study the contribution of water and CO_2, weight losses were divided in three intervals: 50–250, 250–450 and 450–650 °C (Table 2). In the literature, three events have been assigned to these ranges: in the first one, the weight loss is attributed to the removal of physisorbed and interlayer water; in the second interval, the loss is ascribed to the dehydroxylation of the layers and removal of interlayer anions, in this case carbonate; in the last one the weight loss is recognized as the total dehydroxylation, and collapse of the structure due to the removal of the remaining interlayer anions [23].

Regarding the N_2 adsorption isotherms of the LDHs calcined at 550 °C for 4 h, all samples exhibited type IV isotherms which are characteristic of mesoporous materials [24]. Their specific surface areas ranged from 167 to 279 $m^2\,g^{-1}$ (Table 3). No point B was observed in the samples, indicating that a multilayer is formed from the beginning of the adsorption process. Porosity in calcined LDHs is created by two different processes. On one hand, small, intraparticle porosity occurs due to a "cratering" process [25]. On the other hand, the irregular stacking of plate-like particles creates interparticle pores. The size of these interparticle pores depends mainly on the crystal size; interparticle porosity contributes largely to the total pore volume [5,23]. These phenomena account for the bimodal pore size distribution. Average pore sizes are presented in Table 3, as well as pore volumes.

Temperature-programmed reduction profiles of the LDHs showed different behavior depending on their chemical composition. TPR pattern of MgNiAl revealed that the presence of Mg causes a shift of the reduction temperature of Ni^{2+} species towards higher values, when compared to NiO (330 °C) [26] or to a NiAl LDH (780 °C) [27]. This shift is associated with the formation of a NiO–MgO solid solution in which Ni^{2+} ions are stabilized by the MgO-type matrix against reduction and sintering [28,29]. In MgFeAl, the main hydrogen consumption took place at temperatures above 650 °C. MgCuAl was reduced at the lowest temperature, 160 °C. In MgZnAl, no distinct reduction event was detected. The amount of H_2 consumed per gram and per meter square is presented in Table 4. The sample with the largest H_2 consumption was MgCuAl, the consumption of other trimetallic samples is lower, and very similar amongst them.

Table 3
Textural properties of LHDs calcined at 550 °C.

Catalyst	Specific surface area ($m^2\,g^{-1}$)	Pore volume ($cm^3\,g^{-1}$)	Average pore size (Å)	
			I	II
MgAl	254	1.148	36	397
MgFeAl	237	0.623	36	192
MgNiAl	279	0.638	19	121
MgCuAl	200	0.364	34	78
MgZnAl	167	1.198	34	186

Table 4
Amount of desorbed CO_2 in TPD, basic site density, and H_2 consumption in TPR.

Sample	μmol $CO_2\,g^{-1}$	μmol $CO_2\,m^{-2}$	mmol $H_2\,g^{-1}$	mmol $H_2\,m^{-2}$
MgAl	105	0.514706	–	–
MgFeAl	61	0.360947	4.88	0.028876
MgNiAl	89	0.354582	5.8	0.023108
MgZnAl	114	0.622951	4.12	0.022514
MgCuAl	91	0.522989	11	0.063218

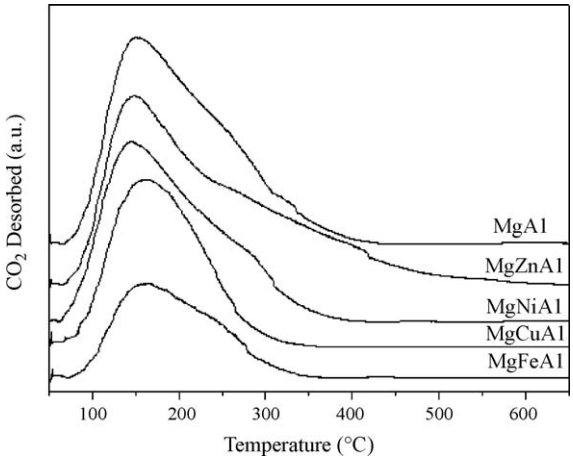

Fig. 3. Temperature-programmed desorption of CO_2 for indicated samples.

CO_2 desorption from the calcined LDHs in the temperature range of 50–650 °C is displayed in Fig. 3. The amount of desorbed CO_2 was calculated from the TPD curves (Table 4). When considering the amount of CO_2 desorbed per gram, it appears that MgAl and MgZnAl have the highest basic strength. However, if the specific surface area is considered, the basic site density of MgAl, MgZnAl and MgCuAl is similar, and much higher than that of MgNiAl and MgFeAl. Therefore, MgCuAl stands out as a solid with relatively high basicity and large reducing capacity.

3.2. Catalytic activity in the 4-methylpentan-2-ol reaction

The rate and selectivity for 4-methylpentan-2-ol conversion reactions were determined at 200 °C. The alcohol is converted on calcined LDHs via two main groups of reactions: dehydrogenation and dehydration. Dehydrogenation of 4-methylpentan-2-ol leads to MIBK as a primary product, and the dehydration reaction produces olefins. A simplified reaction network of the 4-methylpentan-2-ol conversion is shown in Scheme 1.

The catalytic results are shown in Table 5. Reaction rates are initial activities obtained by extrapolating to zero the conversion versus time curves. MgAl showed the lowest reaction rate, with a conversion of 2.87 mol% and 100% selective to the MIBK formation. On LDHs, 4-methylpentan-2-ol conversion rates depend mainly on

Table 5
Conversion, reaction rates and selectivity of 4-methylpentan-2-ol conversion.

Catalyst	Conversion (mol%)	r_a ($\times 10^{-4}$ mol/s g_{metal})	Metal %	Selectivity (mol%)	
				Olefins	MIBK
MgAl	2.87	–	–	–	100
MgFeAl	6.04	0.430	6	39.26	60.75
MgNiAl	19.23	0.980	7	28.22	71.78
MgZnAl	38.79	3.861	7	1.56	98.44
MgCuAl	100	5.358	7	–	100

Note: $T = 200$ °C, W/F = 0.0807 g h g^{-1}_{react}, He/4-methylpentan-2-ol = 39.30 (molar).

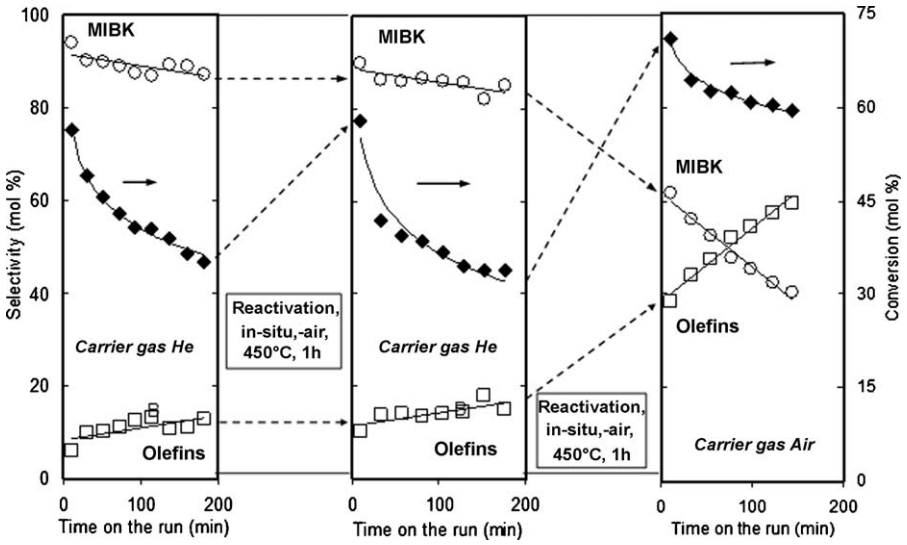

Fig. 4. Catalytic performance of MgZnAl, under helium or air as carrier gas, with 200 min runs, followed by *in situ* reactivation.

the transition metal *Me*. When replacing some of the Al^{3+} by Fe^{3+}, sample MgFeAl, reaction rates and conversion increased; nevertheless, selectivity to MIBK greatly decreased, producing 38.79 mol% olefins. This fact is due to the generation of acidity by the Fe^{3+} cation. This same effect is observed in MgNiAl, producing 28.22% olefins. In MgZnAl and MgCuAl conversion increased greatly, reaching 100% in MgCuAl. These catalysts were also highly selective to MIBK production, with 98.44 and 100 mol%, respectively. These results are well in agreement with TPD-CO_2 and TPR results, as MgZnAl and MgCuAl had the highest basic site density, and MgCuAl also had the greatest reducing capacity.

In order to examine the regeneration capacity of MgZnAl catalyst, at the end of the run, the catalyst was *in situ* regenerated in air at indicated conditions, and a new cycle of evaluation was started, using either He or Air as the carrier gas. The results are shown in Fig. 4. Here, in the first cycle of the experiment, the reaction was carried out under He as a carrier gas, conversion drops from 58 to 35%, while selectivity to MIBK is less affected, after a total of 200 min. This catalyst was reactivated *in situ* in air at 450 °C for 1 h, purged with He, and then a second reaction cycle was started using the same conditions as in the first one. Fig. 4 shows that the second reaction cycle is similar to the first one, pointing out that the deactivation process is a reversible one and may be ascribed to products of the condensation of MIBK. After the second reaction cycle, the catalyst was again reactivated under air at the conditions given above, and a third reaction cycle was started, this time using air as the carrier gas. In this run, the initial selectivity to MIBK dropped considerably, clearly indicating its strong dependence upon the electronic state of Zn. If a redox mechanism were to be operating, then O_2 in air will impede this route to proceed. Note that the sites responsible for the MIBK formation deactivate more rapidly in air than in He (compare the first and the third cycles). Additionally, initial conversion increased, as well as the selectivity to the dehydration products (olefins). It is well known that alcohols are able to reduce transition metal cations to some extent at temperatures as low as 120 °C [30]. In view of the above results, it is clear that Zn cations play a crucial role in turning MgZnAl selective for dehydrogenation and therefore on the mechanism, when operating under reducing conditions (i.e. 4-methylpentan-2-ol/He), but it is particularly hindered when using an oxidative atmosphere (i.e. 4-methylpentan-2-ol/air).

In MgZnAl (Fig. 4) when air is used as carrier gas, Zn^{2+} cations are unable to be reduced or to form Zn–H species, due to oxygen presence, and play a similar role as that of Mg^{2+} cations. Thus, conversion of 4-methylpentan-2-ol follows a mechanism very close to that depicted by Di Cosimo et al., where MgAl-exhydrotalcites, with 0.5–9.0 Mg/Al molar ratios, catalyze the dehydrogenation of primary alcohols to olefins, acetaldehydes and ethers [31,32]. Accordingly, high density of surface Al^{3+}–O^{2-} pairs favors dehydration reactions to form olefins and ethers, while dehydrogenation of primary alcohols, to yield aldehydes, are favored on weak Lewis acid–strong Brönsted base site pairs.

3.3. Proposed reaction mechanism

The product distribution in 4-methylpentan-2-ol conversion reaction is influenced by the surface acid–base properties. Di Cosimo et al., reported that three different types of basic sites exist in MgAl LDH [31]: isolated O^{2-} ions, Mg^{2+}–O^{2-} pairs, and OH groups; their relative concentration depends on the Al content. In

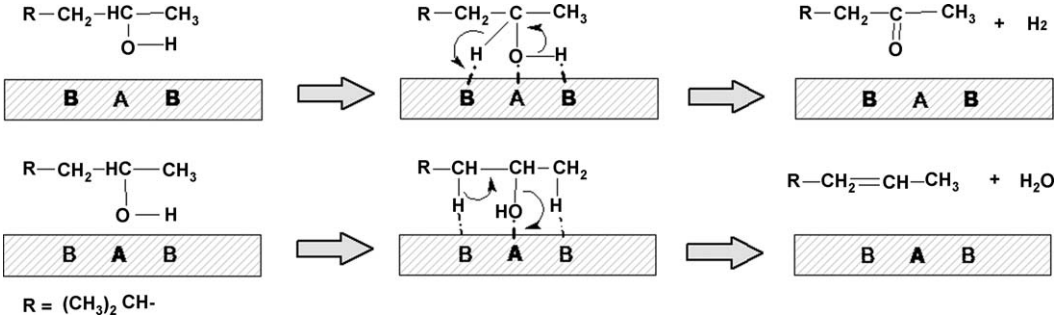

Scheme 2. Proposed reaction mechanism for MIBK formation.

contrast, the surface Lewis acidic sites are provided by Mg^{2+}, Al^{3+} and/or others cations (substitution of Mg or incorporation of Ni^{2+}, Fe^{3+}, Cu^{2+}, and Zn^{2+}). In a general form, the possible MIBK formation mechanism is represented in Scheme 2. Dehydrogenation involves the initial adsorption of 4-methylpentan-2-ol on a strong acid–base pair site, which breaks the O–H bond forming a surface alkoxy intermediate. The rate determining step includes the rupture of the C_α–H_α bond in the alkoxy group due to another strong basic site. Finally, the MIBK product is formed. A similar mechanism was observed by Nondek and Sedlácek in their study with Cr_2O_3 [33]. Bifunctional catalysts usually work under milder conditions than monofunctional ones, their deactivation is much slower and they can perform several steps simultaneously [34].

However, dehydration of alcohols occurs on oxides containing small, highly charged cations which exhibit acidic properties. These properties favor dehydration reactions to form olefins and ethers. Olefin formation is the predominant reaction on acidic oxides [35]. 4-Methylpentan-2-ol dehydration to olefins on mixed oxides proceeds via the E1cB mechanism; this requires both strong basic sites and weak Lewis acid sites [36]. Initially, the adsorption of the 4-methylpentan-2-ol molecule and the O–H bond rupture on the acid–strong base pair site gives rise to a surface alkoxy group. Then, the E1cB mechanism leads to the abstraction of the most acidic proton in the alkoxy intermediate on the basic site, with formation of a carbanion by C_β–H_β bond rupture. Formation of olefins takes place in the final step.

Based on this scheme, as an example, the reaction of dehydrogenation on MgZnAl mixed oxide, using He as a carrier gas, happens in the following way: 4-methylpentan-2-ol dissociatively adsorbs on Mg^{+2} (or Zn^{2+})- O^{2-} pairs (B sites). Hydrogen atom, from the C_α, is removed by Zn^{2+} cation. It is likely that Zn cations directly participate in the abstraction of hydrogen to form surface zinc-hydride, Zn–H, species. Accordingly, adsorbed hydrogen on ZnO has been directly observed by IR, the Zn–H vibration appears at 1705 cm^{-1}, and the O–H at 3490 cm^{-1} [37]. In fact, bond dissociation energy of Zn–H is 85.8 kJ mol^{-1}, 1.5 times lower than that of Mg–H, or 5 times lower that MeO–H. Additionally, Mg–O–Zn or Zn–O offer lower bond dissociation energies than either Al–O or Mg–O bonds, indicating that the former basic O^{2-} sites are more likely to interact with hydrogen atoms of OH groups. Breaking of the C–H_α bond in secondary alcohols, using Cr_2O_3 as a catalyst, has been regarded as the rate limiting step [33]. A similar behavior was observed on the sample containing Cu^{2+} (MgCuAl). In fact, the dehydrogenation route depends on the dissociation of terminal OH bond of the alcohol and the abstraction of the hydrogen by the reducible cations, thus favoring the MIBK production. These results are in agreement with those reported by Sampieri and Lima, where the acid–basic properties of microwave irradiated Mg, Al, Mn and/or Zn-containing LDHs were studied [38].

4. Conclusion

LDHs made up of three cation types, were prepared by a coprecipitation procedure showing pure hydrotalcite-like crystalline phases, which upon annealing at 550 °C turn into Mg(Al*Me*)O solid solutions (except in the case of Cu). The isomorphic incorporation of reducible cations (*Me*) into the layers of LDHs, and later upon calcination into Mg(Al*Me*)O, brings about significant variations in the basicity and acidity, in comparison with that of Mg(Al)O (i.e. the calcination product of typical MgAl-hydrotalcite). Depending on the substituting reducible cation *Me*, LDHs can be tailored to be selective to dehydrogenation or dehydration reactions. The catalytic conversion of 4-methylpentan-2-ol, an acid–base sensible reaction, reflects the variations in bifunctional acid–base properties of *Me* substituted LDHs. For instance, when *Me*: Zn or Cu, calcined LDHs selectively catalyze (98–100 mol%) the dehydrogenation of 4-methylpentan-2-ol to MIBK at high conversion (39–100 mol%). The role of the reducible cation is clear because under air the selectivity to MIBK significantly dropped, indicating a hindering of *Me* reduction. On the other hand, doping LDHs with Ni or Fe turns the catalyst more selective to olefins (promoted by acid sites). Bifunctional catalysts based on *Me*-doped LDHs can be prepared by adjusting the amount and nature of *Me* in a calcined Mg*Me*Al-LDH.

References

[1] F. Cavani, F. Trifirò, A. Vaccari, Catal. Today 11 (1991) 173.
[2] X. Duan, D.G. Evans (Eds.), Layered Double Hydroxides, Struc. & Bonding, vol. 119, Springer-Verlag, Berlin Heidelberg, 2006.
[3] B.F. Sels, D.E. De Vos, P.A. Jacobs, Catal. Rev. 43 (4) (2001) 443.
[4] J. Sánchez-Valente, F. Figueras, M. Gravelle, P. Kumbhar, J. López, J.-P. Besse, J. Catal. 189 (2000) 370.
[5] M. Cantu, E. López-Salinas, J.S. Valente, R. Montiel, Environ. Sci. Technol. 39 (2005) 9715.
[6] F. Kooli, K. Kosuge, A. Tsunashima, J. Mater. Sci. 30 (1995) 4591.
[7] F. Kooli, K. Kosuge, A. Tsunashima, J. Solid State Chem. 118 (1995) 285.
[8] L. Chmierlarz, P. Kustrowski, A. Rafalska-Lasocha, R. Dziembaj, Thermochim. Acta 395 (2003) 225.
[9] P. Berteau, B. Delmon, J.-L. Dallons, A. Van Gysel, Appl. Catal. 70 (1991) 307.
[10] A. Auroux, P. Artizzu, I. Ferino, V. Solinas, G. Leofanti, M. Padovan, G. Messina, R. Mansani, J. Chem. Soc. Faraday Trans. 91 (1995) 3263.
[11] M.G. Cutrufello, I. Ferino, V. Solinas, A. Primavera, A. Trovarelli, A. Auroux, C. Picciau, Phys. Chem. Chem. Phys. 1 (1999) 3369.
[12] A. Auroux, P. Artizzu, I. Ferino, R. Monaci, E. Rombi, V. Solinas, G. Petrini, J. Chem. Soc. Faraday Trans. 92 (1996) 2619.
[13] A. Auroux, P. Artizzu, I. Ferino, R. Monaci, E. Rombi, V. Solinas, Micropor. Mesopor. Mater. 11 (1997) 117.
[14] M.J. Martinez-Ortiz, D. Tichit, P. Gonzalez, B. Coq, J. Mol. Catal. A 201 (2003) 199.
[15] J.S. Valente, E. Lopez-Salinas, M.S. Cantu, F. Hernandez-Beltran, US Patent 2006/0189481 A1 (2006).
[16] S.M. Auer, J.-D. Grunwaldt, R.A. Köppel, A. Baiker, J. Mol. Catal. A 139 (1999) 305.
[17] Y. Ohishi, T. Kawabata, T. Shishido, K. Takaki, Q. Zhang, Y. Wang, K. Nomura, K. Takehira, Appl. Catal. A 288 (2005) 220.
[18] M. del Arco, P. Malet, R. Trujillano, V. Rives, Chem. Mater. 11 (1999) 624.
[19] M.C. Gastuche, G. Brown, M.M. Mortland, Clay Miner. 7 (1967) 177.
[20] G.W. Brindley, S. Kikkawa, Am. Miner. 64 (1979) 836.
[21] U. Olsbye, D. Akporiaye, E. Rytter, M. Rønnekleiv, E. Tangstad, Appl. Catal. A 224 (2002) 39.
[22] T. Yamaoka, M. Abe, M. Tsuji, Mater. Res. Bull. 24 (1989) 1183.
[23] J.S. Valente, M.S. Cantú, J.G.H. Cortez, R. Montiel, X. Bokhimi, E. López-Salinas, J. Phys. Chem. C 111 (2007) 642.
[24] F. Rouquerol, J. Rouquerol, K. Sing, Adsorption by Powders and Porous Solids. Principles, Methodology and Applications, Academic Press, 1999.
[25] W.T. Reichle, S.Y. Kang, D.S. Everhardt, J. Catal. 101 (1986) 352.
[26] S.D. Robertson, B.D. McNicol, J.H. De Bass, S.C. Kloet, J.W. Jenkins, J. Catal. 37 (1975) 424.
[27] F. Trifiro, A. Vaccari, O. Clause, Catal. Today 21 (1994) 185.
[28] R. Villa, C. Cristiani, G. Groppi, L. Lieti, P. Forzatti, U. Cornaro, S. Rossini, J. Mol. Catal. A 637 (2003) 204.
[29] K. Schultze, W. Makowsky, R. Chyzy, R. Dziembaj, G. Geisman, Appl. Clay Sci. 18 (2001) 59.
[30] J.C. Volta, P. Turlier, Y. Trambouze, J. Catal. 34 (1974) 329.
[31] J.I. Di Cosimo, V.K. Díez, M. Xu, E. Iglesia, C.R. Apesteguía, J. Catal. 178 (1998) 499.
[32] J.I. Di Cosimo, C.R. Apesteguía, M.J.L. Gínes, E. Iglesia, J. Catal. 190 (2000) 261.
[33] L. Nondek, J. Sedlácek, J. Catal. 40 (1975) 34.
[34] N. Lavaud, P. Magnoux, F. Alvarez, L. Melo, G. Giannetto, M. Guisnet, J. Mol. Catal. A 142 (1999) 223.
[35] B. Shi, B.H. Davis, J. Catal. 157 (1995) 359.
[36] A. Gervasini, J. Fenyvesi, A. Auroux, Catal. Lett. 43 (1997) 219.
[37] R.J. Kokes, A.I. Dent, Adv. Catal. Relat. Subj. 22 (1972) 1.
[38] A. Sampieri, E. Lima, Langmuir 25 (2009) 3634.